European Journal of Pharmaceutical Sciences 214 (2025) 107287

Contents lists available at ScienceDirect

European Journal of Pharmaceutical Sciences

journal homepage: www.elsevier.com/locate/ejps

Synthesis and in vitro evaluation of polyethylene glycol-treprostinil conjugates for sustained local delivery in pulmonary arterial hypertension

Giuditta Leone [a,c], Bernard Ucakar [a], Frédéric Perros [b], Raphaël Frédérick [c], Rita Vanbever [a,*]

[a] Université catholique de Louvain, Louvain Drug Research Institute (LDRI), Advanced Drug Delivery & Biomaterials (ADDB), Brussels, Belgium
[b] CarMeN Laboratory, INSERM U1060, INRAE U1397, Université Claude Bernard Lyon 1, Pierre-Bénite France
[c] Université catholique de Louvain, Louvain Drug Research Institute (LDRI), Medicinal Chemistry Research Group (CMFA), Brussels, Belgium

ARTICLE INFO

Keywords:
Polymer-drug conjugates
Prodrug
Treprostinil
Polyethylene glycol
Inhalation
Pulmonary arterial hypertension

ABSTRACT

Treprostinil (TRE) is a prostacyclin analogue approved for the treatment of pulmonary arterial hypertension (PAH). Despite its effectiveness, TRE has a short half-life, necessitating frequent or continuous administration to maintain therapeutic levels while minimizing adverse effects. To improve pharmacokinetics and pulmonary targeting of TRE, we designed a series of polyethylene glycol (PEG) ester conjugates for inhalation. The increase in molecular size achieved through polymer conjugation prevents the passive diffusion of TRE across the alveolar-capillary barrier, a common drawback of small, lipophilic drugs delivered to the lungs. The ester bond between TRE and PEG enables a gradual release of the active compound within the alveolar space. TRE was chemically modified with seven different alkyne-bearing linkers and subsequently conjugated to PEG-azide 6 kDa via click chemistry. These linkers were strategically designed to modulate the chemical environment around the cleavable ester bond, allowing for the systematic evaluation of the steric and electronic effects on the stability of the PEG-TRE conjugates. Drug release studies in bronchoalveolar lavage from healthy rats demonstrated that sterically hindered and electronically stabilized linkers significantly slowed the release of TRE. Moreover, conjugate stability was dependent on the enzymes availability, with a higher conjugate-enzyme ratio leading to slower release, suggesting enzyme saturation as a potential mechanism for controlled drug release. Overall, these findings demonstrate a tunable strategy for releasing drugs from polymer-drug conjugates in biological media.

1. Introduction

Pulmonary arterial hypertension (PAH) is a progressive and life-threatening disease characterized by a sustained elevation in mean pulmonary arterial pressure (mPAP $\geq$ 20 mm Hg at rest), measured by right heart catheterization (Humbert et al., 2022). The disease is driven by complex and multifactorial interactions between pulmonary vascular endothelial cells, smooth muscle cells, and fibroblasts, which contribute to the remodeling of the small pulmonary arteries. Endothelial dysfunction is a hallmark of early-stage PAH. It may result from mechanical stress (e.g., shear stress), toxic injuries, inflammatory stimuli, or genetic mutations (such as those in BMPR2, ACVRL1, or EIF2AK4) (Perros et al., 2021; Ranchoux et al., 2015). This dysfunction disrupts the homeostatic balance between vasodilators (e.g., nitric oxide, prostacyclin) and vasoconstrictors (e.g., endothelin-1), as well as between pro- and anti-proliferative signals. The resulting vasoconstriction, inflammation, and overexpression of growth factors promote the proliferation and migration of pulmonary arterial smooth muscle cells (PASMCs) and fibroblasts, leading to vascular remodeling and luminal narrowing (Budhiraja et al., 2004; Chester and Yacoub, 2014). This remodeling establishes a vicious cycle of increased pulmonary vascular resistance, elevated pressure, and further endothelial injury, ultimately leading to right ventricular hypertrophy and failure (Bousseau et al., 2023; Liu and Morrell, 2013). Despite advances in targeted therapies, including endothelin receptor antagonists, phosphodiesterase type 5 inhibitors, and prostacyclin analogues, PAH remains incurable, and the median survival following diagnosis is approximately 2.8 years without treatment, with many patients eventually succumbing to right heart failure (Benyahia et al., 2013; Humbert et al., 2022; Lan et al., 2018)

The currently approved therapies for PAH primarily target symptoms by reducing pulmonary arterial pressure and pulmonary vascular resistance. However, none can reverse the underlying vascular

* Corresponding author at: Université catholique de Louvain, Louvain Drug Research Institute, Advanced Drug Delivery and Biomaterials, Avenue Emmanuel Mounier 73, Brussels 1200, Belgium.
E-mail address: rita.vanbever@uclouvain.be (R. Vanbever).

https://doi.org/10.1016/j.ejps.2025.107287
Received 2 July 2025; Received in revised form 17 September 2025; Accepted 20 September 2025
Available online 21 September 2025

remodeling that characterizes the disease. Among existing treatments, prostacyclin analogues are considered the most effective therapeutic class due to their potent vasodilatory, anti-proliferative, and anti-inflammatory properties (Barnes et al., 2019; Benyahia et al., 2013). Treprostinil (TRE) is a chemically stable prostacyclin analogue extensively used in the management of PAH. It is available in several formulations: inhaled (Tyvaso), subcutaneous and intravenous infusion (Remodulin), and oral extended-release tablets (Orenitram) (Coons et al., 2019; Gessler, 2018). Despite its clinical benefits, the short plasma half-life of TRE (4 h) necessitates frequent dosing or continuous infusion to maintain optimal therapeutic levels (McEvoy et al., 2023). Fluctuations ("peaks and valleys") in plasma concentrations, especially prominent with intermittent dosing, may cause systemic side effects and suboptimal therapeutic outcomes, which are exacerbated by the narrow therapeutic index of TRE (Channick et al., 2012; Kumar et al., 2016; O'Connell et al., 2016).

Pulmonary drug delivery offers distinct advantages compared to other routes of prostacyclin administration. These include direct targeting of the pulmonary vasculature, rapid local therapeutic effects, reduced systemic exposure, minimal risk of infection, and enhanced patient convenience due to the non-invasive and painless mode of administration (Patton et al., 2004). However, small lipophilic molecules such as TRE are rapidly absorbed across the alveolar-capillary barrier into the systemic circulation, which reduces their retention within the lungs and may produce undesired systemic side effects (Patton et al., 2004). Consequently, inhaled TRE requires frequent administration (four times daily) to maintain effective pulmonary concentrations, minimize plasma level fluctuations, and avoid potential adverse effects (McEvoy et al., 2023; Poms and Kingman, 2011).

Systemic drug absorption following inhalation can be minimized by employing delivery systems that enhance lung retention and promote sustained, localized drug release (Loira-Pastoriza et al., 2014). In this regard, conjugating drugs to polymers via esterification represents a promising strategy; increasing the drug molecular weight through polymer conjugation prolongs pulmonary retention, while the gradual enzymatic cleavage of the ester bond enables controlled and sustained release of the active compound directly in the lung tissue (Arpicco et al., 2013; Bayard et al., 2013; Luo et al., 2016; Marasini et al., 2017). Among the available polymeric carriers, polyethylene glycol (PEG) is particularly advantageous due to its excellent biocompatibility, FDA approval for use in food, cosmetics, and pharmaceuticals, a favorable safety profile, and a well-defined linear structure with only chain termini amenable to chemical modification . PEGylation has demonstrated significant clinical success, improving the pharmacokinetics and pharmacodynamics of numerous drugs, and is widely implemented in modern drug delivery systems. To date, several PEGylated therapies have gained clinical approval, including 28 PEGylated protein-based drugs and 5 small-molecule pharmaceuticals (Bayard et al., 2013; Gao et al., 2024; Greenwald, 2001).

In this study, we aimed to develop a water-soluble PEG-TRE prodrug specifically tailored for pulmonary administration in patients with PAH. We conjugated PEG to TRE carboxylic acid, which is essential for its therapeutic activity. This approach forms a prodrug, ensuring that the active moiety is released only upon the gradual hydrolysis of the ester bond, thereby preventing immediate receptor activation and allowing for sustained therapeutic effects. To achieve this, we synthesized a series of PEG-TRE conjugates to systematically evaluate the parameters influencing drug release kinetics. Seven conjugates were obtained via either copper-catalyzed click chemistry (CuAAC) or strain-promoted azide-alkyne cycloaddition (SpAAC). Linear 6 kDa hydroxy PEGs were modified with azide functionalities and then reacted with TRE-modified esters bearing either an alkyne or cyclooctyne moiety. The resulting triazole ring is chemically stable, while the ester linker connecting TRE is designed to undergo enzymatic cleavage within the pulmonary environment. The design of the ester linker is central to the drug release kinetics. Variations in linker hindrance, lipophilicity, and electron density were used to modulate the local environment of the ester bond, thereby tuning its hydrolytic stability and local release rate.

2. Materials and methods

2.1. Materials and instruments

6 kDa PEG with two terminal hydroxyl groups was purchased from Iris Biotech (Marktredwitz, Germany). Treprostinil was purchased from BLDpharm (Shanghai, China). DBCO-PEG4-OH was purchased from Click Chemistry Tools (Arizona, USA). 1-ethyl-3-(3-dimethylamino propyl) carbodiimide (EDC), 4-dimethylaminopyridine (DMAP), tosyl chloride, triethylamine (TEA), dichloromethane, dimethylformamide (DMF), dimethyl sulfoxide (DMSO), acetonitrile, [2-(prop-2-yn-1-yl) phenyl]methanol, undec-10-yn-1-ol, (4-ethynylphenyl) methanol, 1-phenylprop-2-yn-1-ol, prop-2-yn-1-ol, pent-4-yn-2-ol, 1-Naphtoxyacetic acid were either purchased from Sigma Aldrich (Gillingham, UK) or TCI Chemicals (Tokyo, Japan). Sep-Pak C18 cartridges were purchased from Waters (Milford, MA). Porcine liver enzyme was purchased from Sigma Aldrich. Carl Roth Spectra/Por® membranes (Karlsruhe, Germany) were used to carry out all the dialysis work. LC-MS/MS grade acetonitrile and formic acid were purchased from Biosolve (France). Nuclear magnetic resonance (NMR) spectra were recorded on a Bruker 400 MHz spectrometer.

2.2. Chemistry

2.2.1. Synthesis of TRE-alkyne

The alkyne functionality required on TRE was introduced through Steglich esterification between the carboxylic acid on TRE and the hydroxyl group at the end of the four different alkyne-bearing linkers. The linkers used were: [2-(prop-2-yn-1-yl)phenyl]methanol (R1), undec-10-yn-1-ol (R2), (4-ethynylphenyl) methanol (R3), DBCO-PEG4-OH (R4), 1-phenylprop-2-yn-1-ol (R5), prop-2-yn-1-ol (R6), pent-4-yn-2-ol (R7) (Table 1). The general procedure (Fig. 1) involved dissolving TRE (0.05 g, 0.13 mmol, 1 equiv.) and the alcohol R (6 equiv.) in 1 mL DMF under nitrogen. EDC (0.03 g, 0.15 mmol, 1.2 equiv.) and DMAP (0.05 g, 0.38 mmol, 3 equiv.) were added to this mixture. The solution was left stirring at 45 °C overnight. Thin-layer chromatography was used to track reaction progression; the products Rx-TRE were then purified by silica gel chromatography, using ethyl acetate and cyclohexane as mobile phases, or by preparative HPLC. The collected fractions containing the purified product were combined, evaporated, and dried under vacuum. The products were characterized by HPLC-MS.

2.2.2. Synthesis of TRE-DBCO

The DBCO functionality needed on TRE was added by Steglich esterification between the carboxylic acid on TRE and the hydroxyl end of the linker DBCO-PEG4-OH (R4). The procedure involved dissolving TRE (0.02 g, 0.051 mmol, 1 equiv.) and the alcohol R4 (0.104 g, 0.2 mmol, 4 equiv.) in 1 mL of anhydrous DMF under nitrogen. To this mixture, EDC (0.012 g, 0.061 mmol, 1.2 equiv.) and DMAP (0.019 g, 0.154 mmol, 3 equiv.) were added. The solution was left stirring at 45 °C overnight (Fig. 2). The product TRE-R4 was purified by preparative HPLC, and the collected fractions were combined and evaporated to dryness. The product was characterized by HPLC-MS.

2.2.3. Synthesis of PEG-N3

PEG-N_3 was obtained by first activating PEG hydroxyls through tosylation, followed by nucleophilic substitution with azide (Fig. 1). To this end, PEG-OH 6 kDa (0.3 g, 0.05 mmol, 1.0 equiv.) was first freeze-dried and then dissolved in 1 mL anhydrous DCM under nitrogen. The solution was cooled to 0 °C for 15 min, and then tosyl chloride (0.057 g, 0.3 mmol, 6 equiv.) and triethylamine (0.05 mL, 0.3 mmol, 6.0 equiv.) were added. The solution was kept at 0 °C for 2 h, then warmed to room temperature and stirred overnight. The reaction solution was added

Table 1
Schematic illustration of the 7 linkers and the corresponding molecules obtained by esterification of TRE.

TRE	[2-(prop-2-yn-1-yl) phenyl]methanol **R1**	**R1-TRE**
	undec-10-yn-1-ol **R2**	**R2-TRE**
	(4-ethynylphenyl) methanol **R3**	**R3-TRE**
	DBCO-PEG4-OH **R4**	**R4-TRE**
	1-Phenyl-2-propyn-1-ol **R5**	**R5-TRE**
	prop-2-yn-1-ol **R6**	**R6-TRE**
	pent-4-yn-2-ol **R7**	**R7-TRE**

dropwise into 30 mL of cold diethyl ether, repeated three times, to precipitate PEG-tosyl. The precipitate was then dried under vacuum, dissolved in 10 mL of water, and subsequently freeze-dried.

PEG-tosyl (6 kDa, 0.3 g, 0.05 mmol, 1.0 equiv.) was dissolved in anhydrous DMF under a nitrogen atmosphere. Sodium azide (NaN_3, 0.02 g, 0.29 mmol, 10 equiv.) was added to the flask, and the reaction mixture was stirred at 90 °C overnight. The resulting product was precipitated three times in cold diethyl ether, dried under vacuum, and then dissolved in 5 mL of water. Afterwards, it was transferred into a pre-wetted dialysis bag with a 1000 Da cut-off. Dialysis was carried out against deionized water for 24 h to remove excess NaN_3 and DMF; subsequently, the product was freeze-dried.

2.2.4. Synthesis of PEG-TRE conjugates by CuAAC

PEG-N_3 6 kDa (150 mg, 0.025 mmol, 0.5 equiv.), R1-TRE (50.7 mg, 0.1 mmol, 2 equiv.) and N,N,N′,N″,N″-Pentamethyldiethylenetriamine (PMDETA) (100 μl, 0.5 mmol, 15 equiv.) were dissolved in 1.5 mL DMF under nitrogen and degassed for 10 min. In a separate vial, copper

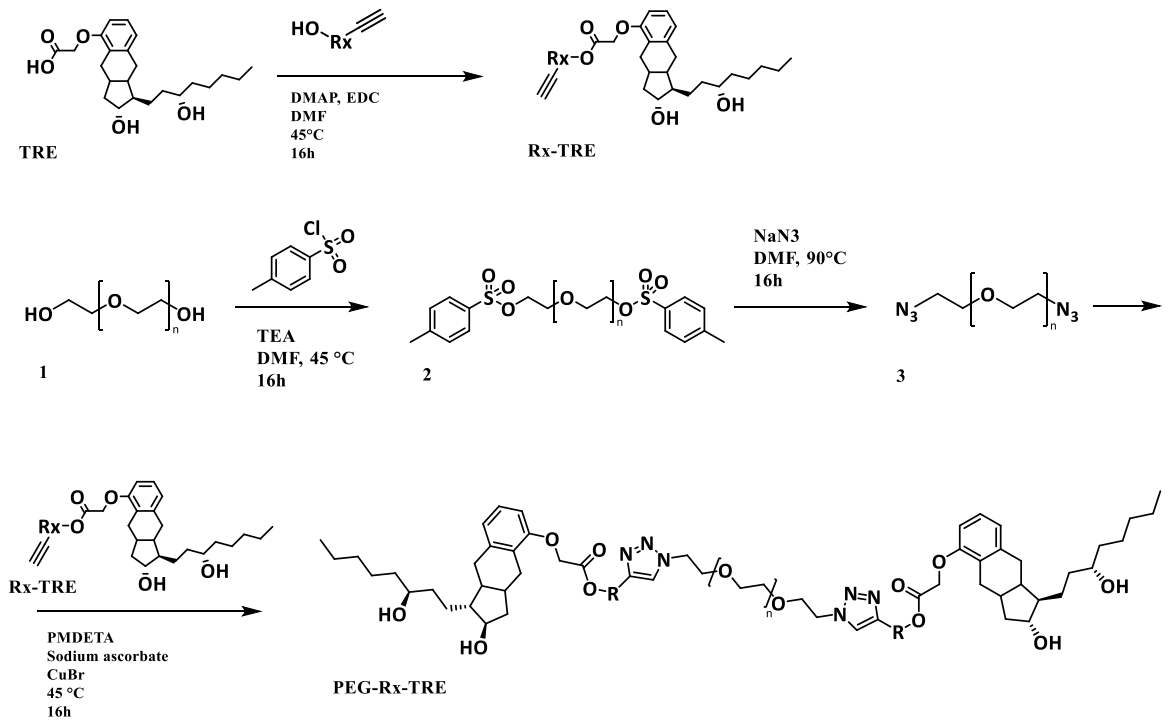

Fig. 1. Copper-catalyzed click chemistry; synthetic route of PEG-TRE conjugates. TRE was modified with alkyne-bearing linkers to obtain Rx-TRE. PEG-N_3 6 kDa (**compound 3**) was synthesized from PEG-OH (**compound 1**) by tosylation (**compound 2**), followed by azidation. Rx-TRE was then conjugated to PEG-N_3 via click chemistry.

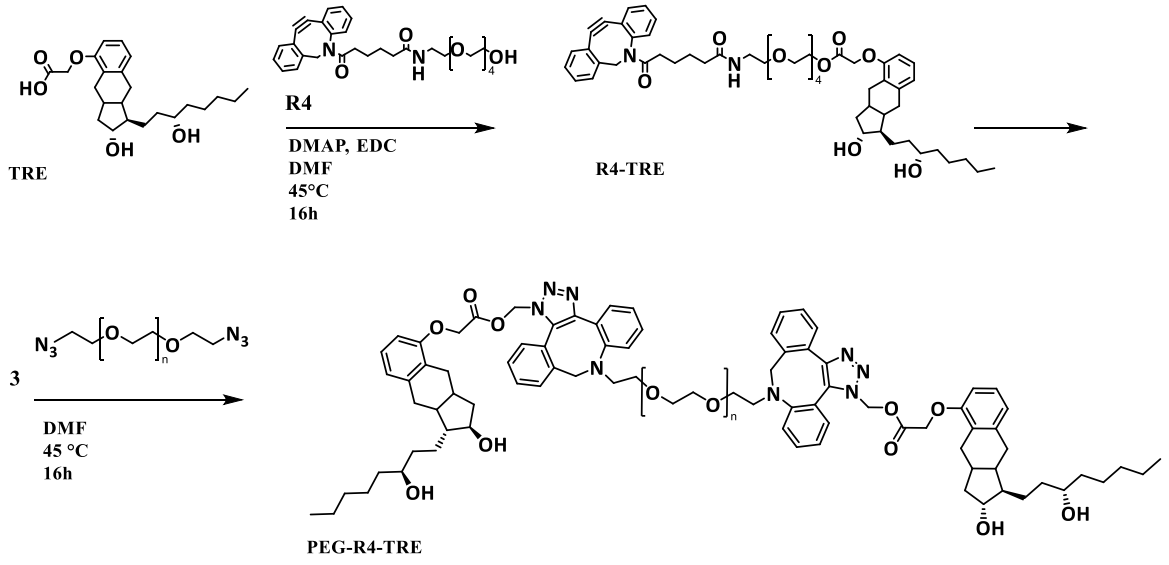

Fig. 2. Strain-promoted azide-alkyne cycloaddition; synthetic route of PEG-TRE conjugates. TRE was modified with DBCO-PEG4-OH (compound R4) to obtain TRE-R4. TRE-R4 was then conjugated to PEG-N3 (compound 3) via click chemistry.

bromide (CuBr) (65 mg, 0.5 mmol, 12 equiv.) and sodium ascorbate (112 mg, 0.6 mmol, 15 equiv.) were dissolved in 1 mL DMF under nitrogen and degassed for 10 min. The CuBr mixture was added to the reaction flask under a nitrogen atmosphere, and the entire solution was degassed for an additional 10 min (Fig. 1). The reaction was stirred at 45 °C overnight. The PEG conjugate was first precipitated in cold diethyl ether and then purified by solid-phase extraction (SPE, Sep-Pak C18) to remove CuBr. The same procedure was applied to the other conjugates.

2.2.5. Synthesis of PEG-TRE conjugate by SPAAC

PEG-N_3 6 kDa (0.019 g, 0.003 mmol, 0.5 equiv.) and R4-TRE (0.016 g, 0.018 mmol, 3 equiv.) were dissolved in 1.5 mL of anhydrous DMF under nitrogen and degassed for 10 min. The reaction was stirred at 45 °C overnight (Fig. 2). The PEG conjugate was purified by precipitation in cold diethyl ether to remove TRE-R4.

2.3. LC-MS/MS method validation in bronchoalveolar lavage

An LC-MS method was validated to ensure the accuracy, precision, and reproducibility of TRE quantification in bronchoalveolar lavage (BAL). Method validation confirms that the analytical procedure reliably detects and quantifies treprostinil in the presence of complex biological

matrices. 1-Naphthoxyacetic acid was selected as an internal standard (IS) due to structural similarity.

2.3.1. Calibration standards and quality control samples

For the standard curves, aliquots of pooled healthy rat bronchoalveolar lavage were obtained from Wistar Rats. Stock solutions of TRE and IS were prepared monthly by dissolution in ethanol and methanol, respectively. These stock solutions were used to prepare working concentrations in BAL, while quality control (QC) stock solutions were prepared from new aliquots of TRE (Nguyen et al., 2021). A constant IS concentration of 300 ng/mL was selected.

2.3.2. Sample preparation

Samples in BAL were prepared and analyzed, or stored at −80 °C. On assay days, 75 µl of ice-cold acetonitrile containing the IS was added to 25 µL of the sample to precipitate the proteins (Ngougni Pokem et al., 2015). The mixture was vortexed for 5 s and then centrifuged at 15,000 × *g* for 10 min. The supernatant was then transferred to glass HPLC vials for analysis.

2.3.3. Chromatography and mass spectrometry method

Optimization of MRM transitions for TRE and IS, as well as LC-MS/MS experiments, was carried out on a Shimadzu LCMS-8040 triple quadrupole mass spectrometer (Shimadzu Corporation, Japan). The system consisted of an LC-20ADXR solvent delivery system, Nexera XR SIL-20AXR autosampler, and CTO-20A column oven. The data processor used was LabSolutions software. Analyses were performed on an Aeris Widepore XB, C18 column (L 50 mm x 2.1 mm, 3.6 µm) (Phenomenex, Torrance, CA, USA). Mobile phase A was 0.1 % formic acid in water, and mobile phase B was 0.1 % formic acid in acetonitrile. All solvents were of LCMS grade. The flow rate was maintained at 0.3 mL/min, and the injection volume was 5 µL. The gradient method employed for the chromatographic separation of TRE and the IS was as follows: the column was pre-equilibrated with a mixture of 95 % A and 5 % B. The mobile phase B was then increased to 95 % over 5 min and held for 4 min. The total runtime was 9 min. The needle and seal wash consisted of 10 % isopropanol. The triple quadrupole LC/MS-MS system was equipped with an electrospray ion source using multiple reaction monitoring (MRM) in negative ion mode. TRE qualifier ion was observed to have a mass-to-charge (*m/z*) transition from 390.1 → 332.4; IS mass-to-charge transition was 202.9 → 144.15. The electrospray ionization parameters were: nebulizing gas flow 3 L/min, drying gas flow 15 L/min; desolvation line temperature 250 °C, heating block temperature 400 °C, interface voltage 4.5 kV.

2.3.4. Lower limit of quantification (LLOQ) determination

The LLOQ is defined as the lowest concentration of TRE that could be quantitatively determined with acceptable accuracy and precision. Five replicate samples at the proposed LLOQ concentration were prepared and analyzed in BAL. Calibration curves (1.95–62.5 ng/mL) plotted the relative response of TRE to the IS versus the concentrations of TRE. The standard curve was analyzed by linear regression without forcing the line through the origin. The accuracy of the standard curve point was determined by back-calculating the concentration and comparing it with the nominal concentration (Gallucci et al., 2024; Health and Services, 2001).

2.3.5. Linearity

The linearity of the method was established by analyzing five non-zero calibration standards, including the LLOQ, spanning the expected range of TRE concentrations. Calibration curves were prepared in triplicate over three separate analytical runs in BAL. Linear regression with $1/x^2$ weighting was used to determine the best fit.

2.3.6. Selectivity and matrix effect

Selectivity was assessed by analyzing five replicates of blank BAL samples. Each blank was injected to ensure that no interference co-eluted with TRE or the IS. Additionally, five zero calibrators (matrix + IS, no TRE) and five TRE LLOQ samples were included to verify the absence of significant signal from matrix components. Five replicates of neat solvent solutions spiked with TRE and IS were also tested.

2.3.7. Accuracy and precision

The reproducibility and repeatability of the method were evaluated after injection of four TRE concentration levels: LLOQ, low LQC, medium MQC, and high HQC. Each level was validated in 3 analytical runs to confirm inter-day accuracy and precision, with an independently prepared standard curve run in triplicate. Five replicates per run were analyzed to confirm intra-day accuracy and precision. Accuracy was expressed as the mean % deviation from the nominal value, and precision was expressed as % CV.

2.3.8. Recovery

Recovery was evaluated by comparing the peak areas of extracted QC samples (LLOQ, MQC, HQC) to post-extraction spiked samples at equivalent concentrations. Each level was assessed in triplicate. The recovery of TRE and the IS was calculated separately, and the consistency across QC levels was used to confirm reliable extraction efficiency.

2.4. Drug loading and solubility

The drug loading was measured by enzymatic hydrolysis of the ester bond formed between TRE and the two ends of PEG, followed by quantification of the free drug by LC-MS/MS. The conjugates, at a concentration of 10 µM, were incubated at 37 °C in a solution of Porcine Liver Enzyme 25 U/mL for 24 h (Basak et al., 2008). A high concentration of the enzyme was employed to ensure full TRE release. After incubation, 100 µl of the conjugate/enzyme solution was treated with 300 µl of ice-cold acetonitrile to precipitate the protein. The samples were then centrifuged at 15,000 × *g* for 10 min before LC-MS/MS analysis.

The solubility of the conjugates was estimated by adding increasing amounts of ultrapure water to freeze-dried conjugates at room temperature until complete dissolution (Arpicco et al., 2013). Solubility was estimated by the volumes added in three parallel experiments.

2.5. Drug release

The rate of hydrolysis of the conjugates was measured in PBS at pH 7.4, in BAL and serum from healthy rats. To obtain BAL, male Wistar rats were euthanized with isoflurane, and 5 mL of Hank's Balanced Salt Solution (HBSS; no Ca^{+2}, no Mg^{+2}, Gibco™, Life Technologies, Gent, Belgium) was injected into the trachea and withdrawn after a few seconds. The BAL was then centrifuged at 4500 × *g* for 10 min to remove the cells, and the supernatant was stored at −80 °C. All experimental procedures were performed in compliance with the guidelines of the Institutional Animal Care and Use Committee of the Université Catholique de Louvain (Permit number: 2023/UCL/MD/45). Efforts were made to minimize animal suffering.

The conjugates were dissolved in PBS to achieve a final concentration of TRE equivalents of 10 µM. In BAL, the concentrations analyzed were 10 µM, 200 µM, and 800 µM TRE equivalents. All the samples were incubated at 37 °C, and at predetermined time points, three times the volume of ice-cold acetonitrile was added to precipitate the proteins. The samples were then centrifuged at 15,000 × *g* for 10 min, and the supernatant was analyzed by LC-MS/MS. The percentages of TRE released were calculated by comparing the amount released with the amount obtained in the drug loading experiments.

2.6. Stability during storage

To assess the long-term stability and optimal storage conditions of

the prepared materials, dry powders and solutions were subjected to accelerated stability testing. Solutions were prepared by dissolving PEG-R7-TRE (17 %; 1.5 % TRE equivalents), mannitol (58 %), and leucine (25 %) in ultrapure water (Banat et al., 2025; Bosquillon et al., 2001). Half of these solutions were freeze-dried to obtain a dry powder. Solutions and dry powders were then incubated at 40 °C for 1 month. Time-zero samples of both dry powders and solutions served as references and were immediately stored at −80 °C until analysis. This accelerated protocol enables the prediction of long-term stability over a shorter timeframe, particularly in early-stage development or preliminary assessments (González-González et al., 2022; Legrand et al., 2021). After one month, the samples were analyzed by LC-MS/MS to measure the amount of free TRE.

3. Results

3.1. Chemistry

PEG-TRE conjugates were synthesized using both copper-catalyzed click chemistry and strain-promoted click chemistry. PEG was activated via tosylation followed by azidation, yielding two azide groups at both termini. For the Cu-catalyzed approach, TRE was modified by esterification with different linkers to introduce an alkyne group and then conjugated to PEG-N_3 through CuBr catalysis (Table 1). In the copper-free approach, TRE was esterified with a dibenzocyclooctyne (DBCO) group, allowing for conjugation to PEG via strain-promoted azide-alkyne cycloaddition (SPAAC), thereby eliminating the need for a metal catalyst.

The seven Rx-TRE esters were characterized by HPLC-MS, identifying the correct *m/z* ratio. **R1-TRE:** chemical formula C34H52O5, Molecular weight: 540.79 g/mol. HRMS ESI found for C34H53O5 $[M+H]^+$541.38. Purity 93 %; Yield 80 %. **R2-TRE:** chemical formula C32H40O5, Molecular weight: 504.29 g/mol. HRMS ESI found for C32H40O5Na $[M+Na]^+$ 527.01. Purity 86 %; Yield 45 %. **R3-TRE:** chemical formula C32H40O5, Molecular weight: 540.71 g/mol. HRMS ESI found for C32H40O5Na $[M+Na]^+$ 527.4. Purity 90 %; Yield 75 %. **R4-TRE:** chemical formula C52H68N2O10, Molecular weight: 881.12 g/mol. HRMS ESI found for C52H68N2O10Na $[M+Na]^+$ 903. Purity 86 %; Yield 75 %. **R5-TRE:** chemical formula C32H40O5, Molecular weight: 540.67 g/mol. HRMS ESI found for C32H40O5Na $[M+Na]^+$ 527.3. Purity 95 %; Yield 60 %. **R6-TRE:** chemical formula C26H36O5, Molecular weight: 428.26 g/mol. HRMS ESI found for C26H36O5Na $[M+Na]^+$ 451.26. Purity 83 %; Yield 56 %. **R7-TRE:** chemical formula C28H40O5, Molecular weight: 456.29 g/mol. HRMS ESI found for C28H40O5 $[M-OH]^-$ 439.21. Purity 93 %; Yield 70 %.

PEG-N_3 was obtained after tosylation and azidation, and the products were characterized by 1H—NMR: **PEG-Tosyl Compound 2**: ^{1}H NMR (400 MHz, $CDCl_3$, δ in ppm) δ 7.79 (d, 4H), δ 7.34 (d, 4H), 4.15 (t, 4H), 3.65 (m, PEG), 2.45 (s, -CH_3). Yield 75–90 %. **PEG-N_3 Compound 3**: ^{1}H NMR (400 MHz, $CDCl_3$, δ in ppm) 3.65 (m, PEG), 3.39 (t, 4H). Yield 70–90 %.

The structure of all the conjugates PEG-Rx-TRE was confirmed by the appearance of the peak with chemical shift δ 8, corresponding to the hydrogen of the triazole ring formed during the click reaction (signal of C-37, Fig. 3C). Moreover, the displacement of the C-3 proton signal in the ^{1}H NMR spectrum, which shifted from δ 4.6 (Fig. 3A) to δ 4.8 (Fig. 3B), indicated the formation of the ester bond. For instance, the formation of TRE-R3 was confirmed by the appearance of characteristic peaks in the ^{1}H NMR spectrum corresponding to the benzyl proton of the R3 linker (signals of C-32, 34, 31, 35, Fig. 3B), as well as the signal of C-29. The appearance of the triazole-ring hydrogen and the shift of the hydrogen adjacent to the ester further characterized this conjugate. Representative NMR data for one conjugate is shown here; the spectra for the remaining six conjugates are available (Figures S1–7, supplementary materials). The final azide conjugates contain a hydrolysable ester bond and a stable triazole linkage between PEG and TRE. The ester bond enables the controlled release of TRE in its active form, while the triazole ensures the stability of the conjugate.

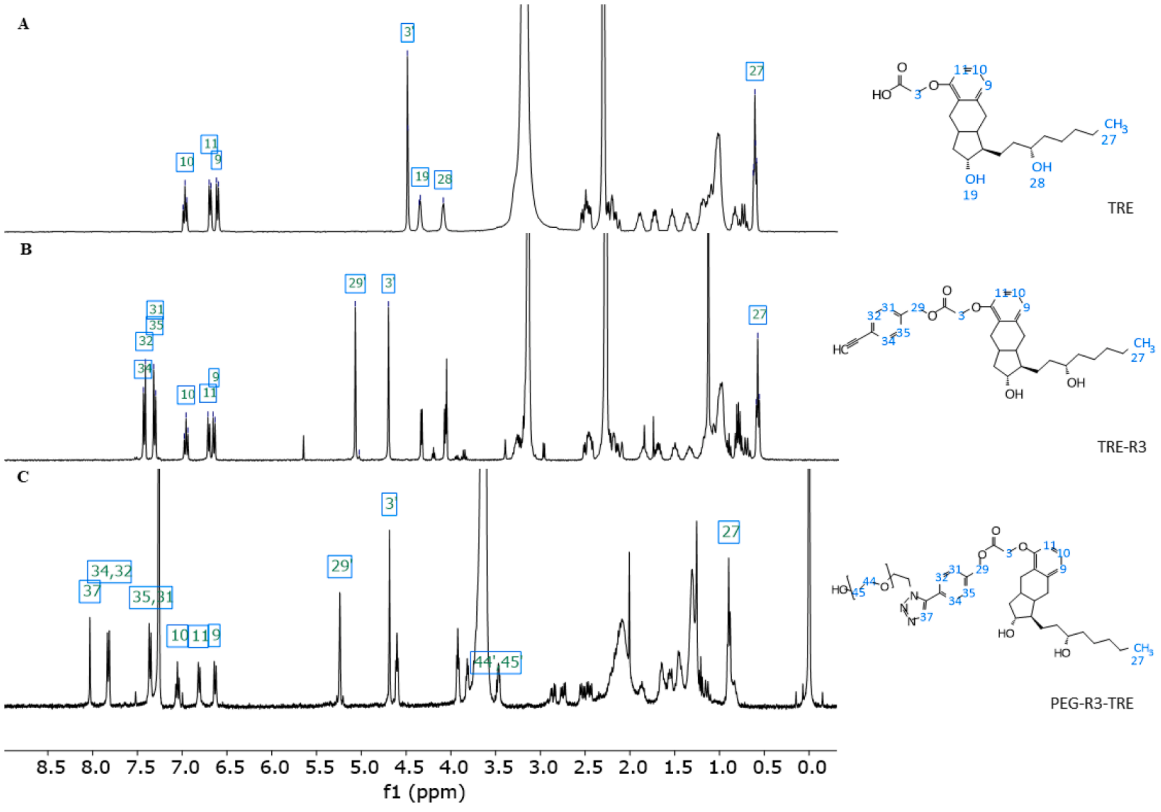

Fig. 3. 1H NMR spectra and chemical structures of TRE, R3-TRE, and PEG-R3-TRE. Relevant hydrogens are highlighted by numbering in spectra and structures.

Compound PEG-R1-TRE: 1H NMR (400 MHz, CDCl3) δ 8.12 (s, 1H), 7.90 (s, 2H), 7.69 (d, $J = 7.6$ Hz, 2H), 7.47 (d, $J = 7.3$ Hz, 3H), 7.41 (t, $J = 7.4$ Hz, 2H), 7.37 (d, $J = 6.5$ Hz, 3H), 7.04 (t, $J = 7.8$ Hz, 2H), 6.79 (d, $J = 7.4$ Hz, 2H), 6.62 (d, $J = 8.3$ Hz, 3H), 5.44 (s, 4H), 4.66 (s, 5H), 4.58 (t, $J = 5.1$ Hz, 5H), 3.64 (s, 545H), 0.89 (t, $J = 6.6$ Hz, 9H). Purity 99.9 %; Yield 19 %. **Compound PEG-R2-TRE**: 1H NMR (400 MHz, CDCl3) δ 7.45 (s, 2H), 7.06 (t, $J = 7.9$ Hz, 2H), 6.80 (d, $J = 7.4$ Hz, 2H), 6.63 (d, $J = 8.2$ Hz, 1H), 4.61 (s, 3H), 4.50 (t, $J = 5.1$ Hz, 3H), 4.18 (t, $J = 6.6$ Hz, 3H), 3.64 (s, 545H), 0.89 (t, $J = 6.4$ Hz, 6H). Purity 99.97 %; Yield 29 %. **Compound PEG-R3-TRE**: 1H NMR (400 MHz, CDCl3) δ 8.03 (s, 3H), 7.82 (d, $J = 8.0$ Hz, 5H), 7.36 (d, $J = 7.9$ Hz, 6H), 7.05 (t, $J = 7.8$ Hz, 3H), 6.81 (d, $J = 7.5$ Hz, 3H), 6.63 (d, $J = 8.3$ Hz, 3H), 5.24 (s, 5H), 4.69 (s, 6H), 4.60 (t, $J = 5.0$ Hz, 5H), 3.64 (s, 545H), 0.89 (d, $J = 7.0$ Hz, 9H). Purity 99.98 %; Yield 46 %. **Compound PEG-R4-TRE:** ^{1}H NMR (400 MHz, $CDCl_3$) δ 7.66 (s, 1H), 7.53 (d, $J = 6.7$ Hz, 1H), 7.45 (d, $J = 6.0$ Hz, 2H), 7.38 (d, $J = 8.1$ Hz, 1H), 7.05 (t, $J = 7.6$ Hz, 1H), 6.98 (dd, $J = 12.3$, 6.3 Hz, 1H), 4.65 (s, 2H), 4.35 (s, 2H), 3.64 (s, 545H), 0.89 (d, $J = 6.8$ Hz, 2H). Purity 100 %; Yield 35 %. **Compound PEG-R5-TRE:** ^{1}H NMR (400 MHz, $CDCl_3$) δ 8.04 (s, 1H), 7.83 (d, $J = 7.8$ Hz, 2H), 7.36 (d, $J = 7.8$ Hz, 2H), 5.24 (s, 2H), 4.69 (s, 2H), 4.61 (t, 2H), 3.65 (d, $J = 1.7$ Hz, 545H), 0.89 (t, $J = 7.2$ Hz, 5H). Purity 100 %; Yield 25.5 %. **Compound PEG-R6-TRE:** ^{1}H NMR (400 MHz, $CDCl_3$) δ 7.79 (s, 1H), 6.77 (d, $J = 7.5$ Hz, 3H), 5.35 (s, 1H), 4.67 (s, 3H), 4.57 – 4.50 (m, 3H), 3.65 (s, 540H), 0.92 (t, $J = 6.4$ Hz 7H). Purity 99.8 %; Yield 30 %. **Compound PEG-R7-TRE:** ^{1}H NMR (400 MHz, $CDCl_3$) δ 7.52 (s, 3H), 7.03 (s, 2H), 5.33 – 5.23 (m, 3H), 4.59 (s, 4H), 4.48 (d, $J = 5.0$ Hz, 5H), 3.65 (s, 545H), 1.32 (s, 6H), 0.89 (d, $J = 6.8$ Hz, 7H). Purity 99.9 %; Yield 21 %.

3.2. LC-MS/MS method validation

TRE standard curves were prepared in bronchoalveolar lavage (BAL) from healthy rats in triplicate. The ratio between the peak area of TRE and the peak area of IS was plotted linearly at a TRE concentration range of 1.95–62.5 ng/mL. The linearity was reproducible, with a regression coefficient > 0.99. The percentage accuracy of the calibration curves ranged from 93 to 104 % (Table S1, supplementary materials). The LLOQ was established at 4 ng/mL, demonstrating a signal-to-noise ratio of ≈ 10, a deviation from the nominal value of <20 %, and a coefficient of variation (CV) < 20 % across replicates. To verify the absence of interference at the retention times of TRE (5.3 min) and IS (4.4 min), extractions from neat solvent and rat BAL preparations were analyzed (Figure S8, supplementary materials). The chromatograms did not present any peaks that interfered with the peaks of interest. For all biological samples, the accuracy and precision intra- and inter-day were 93–103 % and 92–101 %, with CVs between 5 % and 8 % and 6 % and 9 %, respectively (Table S2, supplementary materials). This assay demonstrated that accuracy and precision were acceptable across all samples, indicating that the method is robust enough to generate reproducible data. The procedure for extracting TRE and precipitating proteins from biological samples was proven to be precise and efficient, as the percentage of TRE recovery was consistently 100 % for the three concentrations tested (Table S3, supplementary materials).

3.3. Drug loading and solubility

The drug loading was described as the percentage of treprostinil by weight relative to the total mass of the conjugate (Table 2). The drug loading was assessed in three different analyses of a single production batch and is expressed as mean ± standard deviation. The values obtained ranged between 3 and 11 %. Assuming complete substitution of PEG termini with TRE, the maximum possible drug loading is 11 %, indicating that the PEG-R7-TRE achieved complete substitution. Solubility tests demonstrated that PEGylation of TRE carboxylic acid did not prevent dissolution in water. The predicted solubility of the acid form of TRE in water is 7.3 μg/mL (ALOGPS). Since the water solubility of TRE is low, the pharmaceutical form uses TRE sodium salt, whose solubility is 82 mg/mL (experimental value Selleck Chemicals, Texas, USA). Therefore, despite the loss of the carboxylic acid functional group, the water solubility of all the conjugates remained satisfactory (Table 2).

Table 2
Solubility and drug loading data for all the PEG-TRE conjugates.

Conjugate	Drug Loading (%)	Conjugate solubility (mg/mL)	Soluble TRE equivalents (mg/mL)
PEG-R1-TRE	5.7 ± 0.2	79 ± 7	5.4 ± 0.6
PEG-R2-TRE	9.0 ± 0.8	48 ± 4	5.0 ± 0.4
PEG-R3-TRE	5.0 ± 0.6	114 ± 6	6.1 ± 0.2
PEG-R4-TRE	6 ± 1	101 ± 8	5.9 ± 0.4
PEG-R5-TRE	3 ± 1	101 ± 10	2.6 ± 0.3
PEG-R6-TRE	6 ± 1	115 ± 8	5.6 ± 1.0
PEG-R7-TRE	11 ± 2	102 ± 21	13.3 ± 0.7

Means ± SD are given. $N = 3$, $n = 1$

3.4. Drug release

In vitro release studies of PEG-treprostinil conjugates were conducted in PBS and BAL fluid at 37 °C for 7 days and 24 h, respectively. Additionally, release studies were performed in rat serum, where TRE was quickly cleaved. The conjugates were incubated at an initial concentration of 10 μM (TRE equivalents).

As shown in Fig. 4, the release profiles in PBS and BAL, expressed as the percentage of released TRE, varied considerably among the different conjugates. The conjugates showed moderate stability in PBS pH 7.4 (Fig. 4A): most of them released up to 50 % of TRE after 7 days of incubation, while PEG-R6-TRE and PEG-R7-TRE remained stable, with a maximum of 20 % of free TRE released after 7 days.

TRE release from the conjugates was faster in BAL than in PBS, due to the presence of hydrolytic enzymes (Fig. 4B). At the 2-hour time point, PEG-R1-TRE, -R2, -R3, -R4, -R5 demonstrated rapid initial hydrolysis, with approximately 80–95 % of total TRE released from the conjugates. Conversely, PEG-R6-TRE and PEG-R7-TRE exhibited significantly higher stability, releasing only 20–30 % of the initial TRE at 2 h. By 24 h, all the conjugates were completely hydrolyzed except for PEG-R6-TRE and PEG-R7-TRE, which released 75 % and 55 % of the total conjugated TRE. In rat serum, the conjugates showed little stability, with a quick and burst release of TRE upon incubation (Figure S9, supplementary materials).

Furthermore, a pronounced concentration-dependent effect on hydrolysis rates was observed for almost all conjugates in BAL (Fig. 5, A-G). Conjugates were incubated in BAL at concentrations of 10, 200, or 800 μM (TRE equivalents), and the percentage of released TRE was measured over 24 h. For most conjugates, higher initial concentrations led to markedly slower degradation. For PEG-R1-TRE, -R2, -R3, -R4, -R5, the percentage of TRE released differed greatly between the three concentrations tested. At the 2-hour time point, PEG-R1-TRE (Fig. 5A) released 100 % of TRE when incubated at 10 μM, 95 % at 200 μM, and 65 % at 800 μM. Similarly, PEG-R3-TRE (Fig. 5C) released 92 % of TRE when incubated at 10 μM, 45 % at 200 μM, and 19 % at 800 μM. This behavior was less prominent for PEG-R6-TRE and PEG-R7-TRE, which already demonstrated higher stability at lower concentrations. PEG-R6-TRE (Fig. 5F) released 23 % of TRE at 10 μM, 19 % at 200 μM, and 30 % at 800 μM. In line with the latter, PEG-R7-TRE (Fig. 5G) released 33 % of TRE at 10 μM, 28 % at 200 μM, and 20 % at 800 μM, showing consistent stability across the tested conditions. Overall, the conjugate PEG-R7-TRE was selected as the most promising, showing high drug loading, high stability in BAL, and limited dependence on the conjugate-enzyme

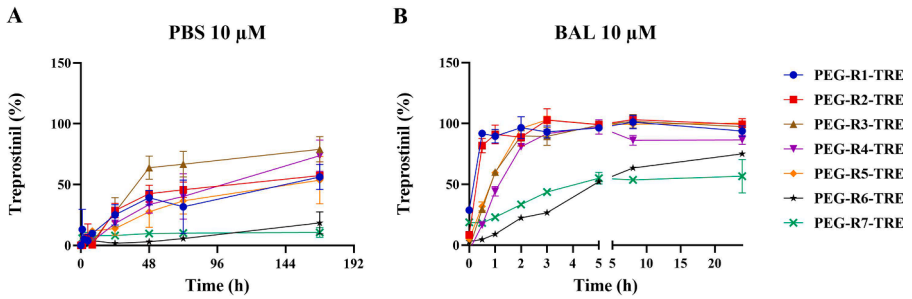

Fig. 4. Stability profile of all conjugates after incubation in A) PBS pH 7.4 and B) bronchoalveolar lavage (BAL) at a concentration of 10 µM (TRE equiv).

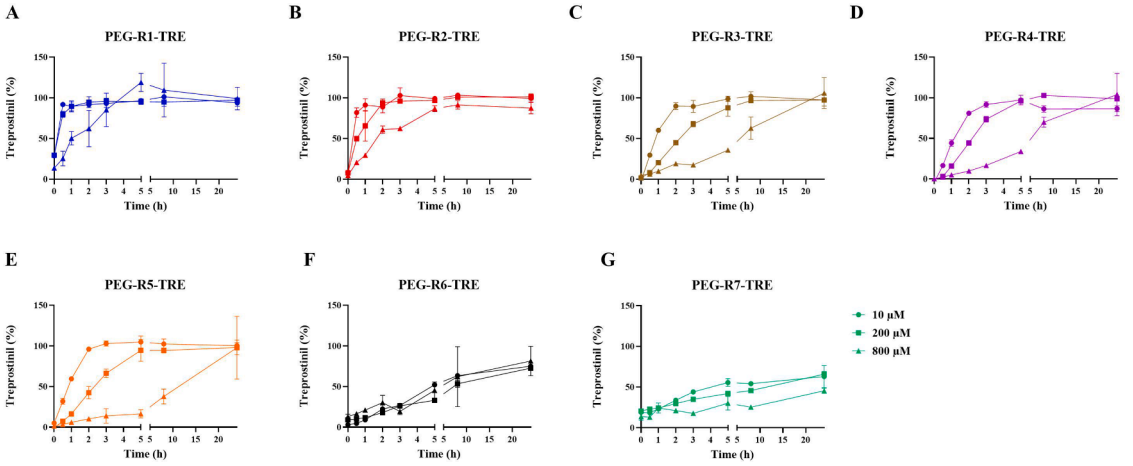

Fig. 5. Stability of the PEG-TRE conjugates after incubation in bronchoalveolar lavage for 24 h. Each graph shows the stability of a single conjugate at different concentrations.

ratio.

3.5. Stability during storage

The conjugate PEG-R7-TRE was tested under accelerated conditions to assess the long-term stability during storage in two pharmaceutical forms: solution and dry powder. The two preparations were compared to unconjugated TRE tested in the same conditions. After 1 month at 40 °C, the PEG-TRE conjugate did not show any sign of degradation when in dry powder form, while the expected hydrolysis of the polymer-drug ester bond was observed in solution (Fig. 6).

4. Discussion

In this study, we successfully synthesized seven distinct polymer–drug conjugates, varying only in the nature of the linker between the active moiety and the polymer. The methodology employed for the synthesis of PEG-TRE conjugates demonstrates remarkable versatility, extending its application beyond the specific drug-polymer combination investigated in this study. This approach leverages the ubiquity of carboxylic acid or hydroxyl functionalities in drug molecules and polymers, allowing for their efficient conjugation through the strategic use of bifunctional linkers. The vast array of commercially available and synthetically accessible linkers, which contain both a carboxylic acid or hydroxyl group and an alkyne moiety, provides flexibility in tailoring the conjugation chemistry. Consequently, this strategy holds promise as

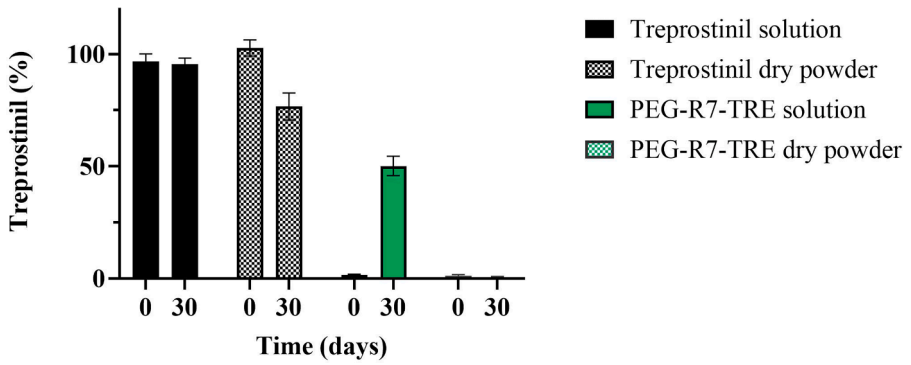

Fig. 6. Quantification of free TRE in solution or dry powder formulations of unconjugated TRE and PEG-R7-TRE subject to accelerated stability testing at 40 °C for 1 month.

a broadly applicable platform for developing next-generation drug delivery systems.

The choice of PEG offers several advantages, particularly in the context of pulmonary administration. The increase in hydrodynamic size of the conjugated drug enables prolonged retention within the lung environment, and the hydrophilic nature of the polymer allows for solubilization of lipophilic therapeutic agents.

The observed differences in release rates of free TRE from PEG conjugates in BAL strongly indicate that the inherent physicochemical characteristics of the linker play a critical role in dictating their stability. Specifically, conjugates PEG-R1-, PEG-R2-, PEG-R3-, PEG-R4-, and PEG-R5-TRE were quickly hydrolyzed, whereas PEG-R6-TRE and PEG-R7 exhibited slower release of the active compound over the 24-hour incubation period. These differences can be attributed to a complex interplay of electronic effects, lipophilicity, and steric hindrance within the linker structure, which impacts the susceptibility of the ester bond to enzymatic hydrolysis (Nguyen, 2022; Takahashi, 2021). The physicochemical characteristics of the linkers are summarized in Table 3. The nature of the leaving group determines the electronic effects exerted by the linker on the ester bond. The LogP assesses the lipophilicity of the environment at the hydrolysis site, and the Van der Waals surface area and solvent-accessible surface area quantify the steric hindrance. The release rate was significantly correlated with linker LogP, Van der Waals, and solvent accessible surface areas in both BAL and PBS (Fig. 7 and Figure S10, supplementary materials). Regarding electronic effects, the nature of the leaving group influences the rate of ester hydrolysis (Table 3). Conjugates incorporating alkyl-derived linkers, such as PEG-R6-TRE and PEG-R7-TRE, form poor alkoxide leaving groups upon hydrolysis and are therefore less susceptible to ester cleavage. In contrast, conjugates with aryl-derived linkers —such as PEG-R1-TRE, -R3, and -R5— undergo more rapid hydrolysis due to the formation of stabilized phenoxide leaving groups. This highlights the importance of strategic linker chemistry design, considering both the environment around the susceptible bond and the electronic properties of the leaving group to achieve the desired controlled drug release in biological environments.

The lipophilicity of the linker, expressed as LogP, played a role in influencing the stability of the conjugates: conjugates with higher lipophilicity showed a quicker release of the active drug. An explanation for this behavior might be found in the accessibility of the lipophilic ester site to other types of enzymes, such as lipases, making the conjugate susceptible to cleavage by multiple enzymes.

PEG-R6-TRE, which demonstrated high stability, features the smallest linker in terms of both Van der Waals (92 Å^2) and solvent-accessible surface area (202 Å^2) among all tested conjugates. This steric bulk likely provides significant protection to the ester bond, making it less accessible to enzymatic cleavage. Similarly, PEG-R7-TRE also benefits from its comparatively compact alkyl structure (Van der Waals: 151 Å^2, Solvent accessible: 247 Å^2) compared to the aryl-containing linkers. When comparing the less stable aryl-derived conjugates (R1, R3, R5), their generally larger solvent-accessible surface areas (>280 Å^2) further contribute to their susceptibility by offering less steric protection against enzymatic attack. Even for PEG-R2-TRE, despite its alkyl nature, its exceptionally large solvent-accessible surface area (>440 Å^2) likely contributes to its rapid degradation, indicating that a combination of electronic and steric factors dictates the overall stability profile

Table 3
Calculated physicochemical and structural descriptors of Rx linkers.

#Linker	Linker's name (IUPAC)	Rx-TRE structure	[d] Leaving group	[a]LogP	[b]Van der Waals surface area Å^2	[b]Solvent accessible surface area Å^2
R1	[2-(prop-2-yn-1-yl)phenyl]methanol	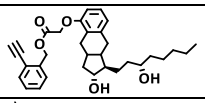	+++	2.04	229	309
R2	undec-10-yn-1-ol	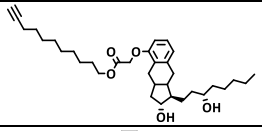	+	3.14	337	442
R3	(4-ethynylphenyl) methanol	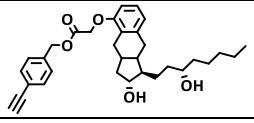	+++	1.62	199	301
R4	DBCO-PEG4-OH	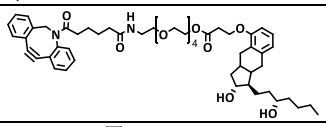	++	0.93	ND[c]	ND
R5	1-phenylprop-2-yn-1-ol	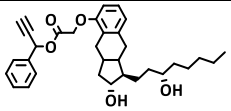	+++	1.66	194	287
R6	prop-2-yn-1-ol	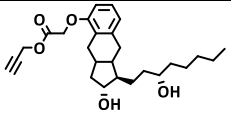	+	-0.06	92	202
R7	pent-4-yn-2-ol	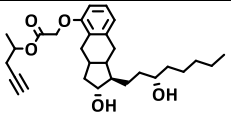	+	0.54	151	247

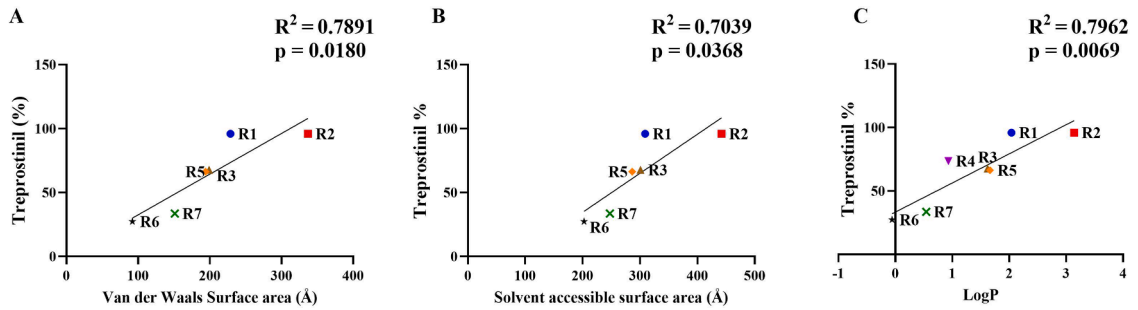

Fig. 7. Influence of A) Van der Waals surface area, B) solvent accessible surface area, and C) LogP on the % of treprostinil released after 3 h of incubation in bronchoalveolar lavage. These results were analyzed by Pearson correlation. Regression lines, correlation coefficients and p-values are added on the graphs.

(Fig. 7).

Beyond the intrinsic properties of the linker, the stability of the PEG-TRE conjugates was also strongly influenced by their initial concentration in BAL fluid. Across all conjugates, increasing the concentration from 10 μM to 200 μM and then to 800 μM consistently resulted in proportionally greater stability, as indicated by slower TRE release rates (Fig. 5). This concentration-dependent effect is consistent with enzymatic saturation described by Michaelis-Menten kinetics. At low substrate concentrations, the esterase enzymes in the BAL fluid are abundant relative to the conjugate and can efficiently catalyze hydrolysis. As the conjugate concentration increases, the enzymes become saturated, resulting in a reduction in the hydrolysis rate per unit of substrate. As a result, a larger proportion of the prodrug remains intact over time because the enzymes are operating at or near their maximum capacity and cannot efficiently process the excess of substrate. However, it is essential to note that the BAL is a large dilution of the epithelial lining fluid and does not represent the entire complexity of the enzymatic landscape of the lungs (Rennard et al., 1986). The obtained in vitro stability may therefore be an overestimation of the stability of these conjugates in vivo, where the enzymatic content is 100 times more concentrated (Fernandes and Vanbever, 2009).

A second possible explanation for the decreased rate of hydrolysis at higher polymer-drug conjugate concentration is increased solution viscosity. A more viscous microenvironment can impede the diffusion of the enzyme and reduce the accessibility of the ester bond. This reduction in molecular mobility of the enzyme slows down the overall catalytic process, thereby decreasing the effective hydrolysis rate. These findings open up promising avenues for future formulation design and provide a tunable platform for drug delivery based on both molecular architecture and dosing strategy.

In line with our study, Nguyen et al. synthesized PEG-paclitaxel ester conjugates and modulated paclitaxel release by varying the steric hindrance of the chemical group adjacent to the cleavable ester bond (Nguyen et al., 2020, 2022). The demonstration that steric hindrance can be tuned to control drug release was novel. However, their study was limited to this single characteristic of the linker. By contrast, linker stability and drug release kinetics are complex phenomena influenced by multiple factors, including the linker's length, its overall chemical composition and its susceptibility to various enzymatic pathways.

Although other TRE prodrugs have been described, this is the first to employ a polymer that both preserves water solubility and prolongs pulmonary residence time. Insmed is developing a TRE prodrug, called treprostinil-palmitil (TPIP), which recently completed a Phase II clinical trial. In this dry-powder formulation, the TRE carboxylic group is covalently linked to a 16-carbon (hexadecyl) chain via an ester bond (Corboz et al., 2017; Leifer et al., 2018). This specific chemical modification is strategically designed to enable once-daily inhaled administration, during which time the ester bond is slowly hydrolyzed in the lungs, mostly by lipase (Nguyen et al., 2024). Despite showing tremendous improvement in pharmacokinetics (Ismat et al., 2022), TPIP's high lipophilicity (LogP > 9) presents particular challenges in its development and behavior as a prodrug. Highly lipophilic compounds, when introduced into the aqueous environment of the lung lining fluid, can remain undissolved (Guo et al., 2021). Undissolved particles can negatively impact the kinetics of drug release. In addition, alveolar macrophages are highly efficient at clearing lipophilic foreign particles from the respiratory tract (Little et al., 2025; Patel et al., 2015).

To conclude, our systematic investigation into the physicochemical properties of linkers and their effects on TRE release from conjugates provides valuable insights and practical guidance for future polymer prodrug development. Its principles could be applied to other small-molecule drugs and routes of drug administration beyond inhalation.

CRediT authorship contribution statement

Giuditta Leone: Writing – original draft, Validation, Methodology, Investigation, Formal analysis, Data curation. **Bernard Ucakar:** Investigation. **Frédéric Perros:** Writing – review & editing, Funding acquisition, Conceptualization. **Raphaël Frédérick:** Writing – review & editing, Supervision, Resources. **Rita Vanbever:** Writing – review & editing, Supervision, Resources, Project administration, Methodology, Funding acquisition, Formal analysis, Conceptualization.

Funding

This work was supported by the Fonds National de la Recherche Scientifique (FNRS, Belgium; grant number PC01120F). Rita Vanbever is Research Director of the FNRS.

Supplementary materials

Supplementary material associated with this article can be found, in the online version, at doi:10.1016/j.ejps.2025.107287.

Data availability

Data will be made available on request.

References

Arpicco, S., et al., 2013. Preparation and characterization of novel poly(ethylene glycol) paclitaxel derivatives. Int. J. Pharm. 454, 653–659. https://doi.org/10.1016/j.ijpharm.2013.05.027.

Banat, H., et al., 2025. Comprehensive aerodynamic and physicochemical stability evaluations of nanocrystal-based dry powder inhalers: the role of mannitol and leucine in enhancing performance. Pharmaceutics 17. https://doi.org/10.3390/pharmaceutics17040436.

Barnes, H., et al., 2019. Prostacyclin for pulmonary arterial hypertension. Cochrane Database Syst. Rev. 5. https://doi.org/10.1002/14651858.CD012785.pub2. CD012785.

Basak, A., et al., 2008. Studies on the porcine liver esterase-catalyzed hydrolysis of pentaacetyl catechin and epicatechin: application to the synthesis of novel dimers and trimers. Bioorg. Med. Chem. Lett. 18, 4900–4903. https://doi.org/10.1016/j.bmcl.2008.07.058.

Bayard, F.J., et al., 2013. Polyethylene glycol-drug ester conjugates for prolonged retention of small inhaled drugs in the lung. J. Control Release 171, 234–240. https://doi.org/10.1016/j.jconrel.2013.07.023.
Benyahia, C., et al., 2013. A comparative study of PGI2 mimetics used clinically on the vasorelaxation of human pulmonary arteries and veins, role of the DP-receptor. Prostaglandins. Other Lipid Mediat. 107, 48–55. https://doi.org/10.1016/j.prostaglandins.2013.07.001.
Bosquillon, C., et al., 2001. Influence of formulation excipients and physical characteristics of inhalation dry powders on their aerosolization performance. J. Control Release 70, 329–339. https://doi.org/10.1016/s0168-3659(00)00362-x.
Bousseau, S., et al., 2023. Pathophysiology and new advances in pulmonary hypertension. BMJ Med. 2, e000137. https://doi.org/10.1136/bmjmed-2022-000137.
Budhiraja, R., et al., 2004. Endothelial dysfunction in pulmonary hypertension. Circulation 109, 159–165. https://doi.org/10.1161/01.CIR.0000102381.57477.50.
Channick, R.N., et al., 2012. Inhaled treprostinil: a therapeutic review. Drug Devel. Ther. 6, 19–28. https://doi.org/10.2147/DDDT.S19281.
Chester, A.H., Yacoub, M.H., 2014. The role of endothelin-1 in pulmonary arterial hypertension. Glob. Cardiol. Sci. Pr. 62–78. https://doi.org/10.5339/gcsp.2014.29, 2014.
Coons, J.C., et al., 2019. Pulmonary arterial hypertension: a pharmacotherapeutic update. Curr. Cardiol. Rep. 21. https://doi.org/10.1007/s11886-019-1235-4.
Corboz, M.R., et al., 2017. Preclinical pharmacology and pharmacokinetics of inhaled hexadecyl-treprostinil (C16TR), a pulmonary vasodilator prodrug. J. Pharmacol. Exp. Ther. 363, 348–357. https://doi.org/10.1124/jpet.117.242099.
Fernandes, C.A., Vanbever, R., 2009. Preclinical models for pulmonary drug delivery. Expert. Opin. Drug Deliv. 6, 1231–1245. https://doi.org/10.1517/17425240903241788.
Gallucci, G.M., et al., 2024. Quantification of treprostinil concentration in rat and human using a novel validated and rapid liquid chromatography-tandem mass spectrometry method: experimental and clinical applications in ischemia-reperfusion injury. Clin. Chim. Acta 561, 119837. https://doi.org/10.1016/j.cca.2024.119837.
Gao, Y., et al., 2024. PEGylated therapeutics in the clinic. Bioeng. Transl. Med. 9. https://doi.org/10.1002/btm2.10600.
Gessler, T., 2018. Inhalation of repurposed drugs to treat pulmonary hypertension. Adv. Drug Deliv. Rev. 133, 34–44. https://doi.org/10.1016/j.addr.2018.06.003.
González-González, O., et al., 2022. Drug stability: ICH versus accelerated predictive stability studies. Pharmaceutics. 14, 2324. https://doi.org/10.3390/pharmaceutics14112324.
Greenwald, R.B., 2001. PEG drugs: an overview. J. Control Release 74, 159–171. https://doi.org/10.1016/s0168-3659(01)00331-5.
Guo, Y., et al., 2021. Pharmaceutical strategies to extend pulmonary exposure of inhaled medicines. Acta Pharm. Sin. B 11, 2565–2584. https://doi.org/10.1016/j.apsb.2021.05.015.
Health, U.D.o., Services, H., 2001. Guidance for industry, bioanalytical method validation. http://www.fda.gov/cder/guidance/4252fnl.pdf.
Humbert, M., et al., 2022. 2022 ESC/ERS guidelines for the diagnosis and treatment of pulmonary hypertension. Eur. Heart. J. 43, 3618–3731. https://doi.org/10.1093/eurheartj/ehac237.
Ismat, F.A., et al., 2022. Safety, tolerability, and pharmacokinetics of treprostinil palmitil inhalation powder for pulmonary hypertension: a phase 1, randomized, double-blind, single- and multiple-dose study. Adv. Ther. 39, 5144–5157. https://doi.org/10.1007/s12325-022-02296-x.
Kumar, P., et al., 2016. A comprehensive review of treprostinil pharmacokinetics via four routes of administration. Clin. Pharmacokinet. 55, 1495–1505. https://doi.org/10.1007/s40262-016-0409-0.
Lan, N.S.H., et al., 2018. Pulmonary arterial hypertension: pathophysiology and treatment. Diseases. 6. https://doi.org/10.3390/diseases6020038.
Legrand, P., et al., 2021. Accelerated stability Assessment Program to predict long-term stability of drugs: application to ascorbic acid and to a cyclic hexapeptide. AAPS. PharmSciTech. 22, 234. https://doi.org/10.1208/s12249-021-02121-8.
Leifer, F.G., et al., 2018. Inhaled treprostinil-prodrug lipid nanoparticle formulations provide long-acting pulmonary vasodilation. Drug Res. (Stuttg) 68, 605–614. https://doi.org/10.1055/s-0044-100374.
Little, I., et al., 2025. Alveolar macrophages: guardians of the alveolar lipid galaxy. Curr. Opin. Lipidol. 36, 153–162. https://doi.org/10.1097/MOL.0000000000000987.
Liu, D., Morrell, N.W., 2013. Genetics and the molecular pathogenesis of pulmonary arterial hypertension. Curr. Hypertens. Rep. 15, 632–637. https://doi.org/10.1007/s11906-013-0393-9.
Loira-Pastoriza, C., et al., 2014. Delivery strategies for sustained drug release in the lungs. Adv. Drug Deliv. Rev. 75, 81–91. https://doi.org/10.1016/j.addr.2014.05.017.
Luo, T., et al., 2016. Synthesis and In vitro evaluation of polyethylene glycol-paclitaxel conjugates for lung cancer therapy. Pharm. Res. 33, 1671–1681. https://doi.org/10.1007/s11095-016-1908-2.
Marasini, N., et al., 2017. Polymer-drug conjugates as inhalable drug delivery systems: a review. Curr. Opin. Colloid. Interface Sci. 31, 18–29. https://doi.org/10.1016/j.cocis.2017.06.003.
McEvoy, C., et al., 2023. Tyvaso DPI: drug-device characteristics and patient clinical considerations. Pulm. Pharmacol. Ther. 83, 102266. https://doi.org/10.1016/j.pupt.2023.102266.
Ngougni Pokem, P., et al., 2015. Validation of a HPLC-MS/MS assay for the determination of total and unbound concentration of temocillin in human serum. Clin. Biochem. 48, 542–545. https://doi.org/10.1016/j.clinbiochem.2015.02.006.
Nguyen, A., et al., 2020. Utilization of click chemistry to study the effect of poly (ethylene)glycol molecular weight on the self-assembly of PEGylated gambogic acid nanoparticles for the treatment of rheumatoid arthritis. Biomater. Sci. 8, 4626–4637. https://doi.org/10.1039/d0bm00711k.
Nguyen, A., et al., 2022. Chemically engineering the drug release rate of a PEG-paclitaxel conjugate using click and steric hindrance chemistries for optimal efficacy. Biomaterials 289, 121735. https://doi.org/10.1016/j.biomaterials.2022.121735.
Nguyen, T., et al., 2024. Treprostinil palmitil inhalation powder leverages endogenous lung enzymes to provide sustained treprostinil. Expert. Opin. Drug Deliv. 21, 1297–1305. https://doi.org/10.1080/17425247.2024.2395444.
Nguyen, T.T., et al., 2021. Development and validation of a bioanalytical LC-MS/MS method for simultaneous determination of sirolimus in porcine whole blood and lung tissue and pharmacokinetic application with coronary stents. Molecules. 26. https://doi.org/10.3390/molecules26020425.
O'Connell, C., et al., 2016. Comparative safety and tolerability of prostacyclins in pulmonary hypertension. Drug Saf. 39, 287–294. https://doi.org/10.1007/s40264-015-0365-x.
Patel, B., et al., 2015. Particle engineering to enhance or lessen particle uptake by alveolar macrophages and to influence the therapeutic outcome. Eur. J. Pharm. Biopharm.: Off. J. Arbeitsgemeinschaft fur Pharm. Verfahrenstechnik e.V 89, 163–174. https://doi.org/10.1016/j.ejpb.2014.12.001.
Patton, J.S., et al., 2004. The lungs as a portal of entry for systemic drug delivery. Proc. Am. Thorac. Soc. 1, 338–344. https://doi.org/10.1513/pats.200409-049TA.
Perros, F., et al., 2021. Smouldering fire or conflagration? An illustrated update on the concept of inflammation in pulmonary arterial hypertension. Eur. Respir. Rev. 30. https://doi.org/10.1183/16000617.0161-2021.
Poms, A., Kingman, M., 2011. Inhaled treprostinil for the treatment of pulmonary arterial hypertension. Crit. Care Nurse 31. https://doi.org/10.4037/ccn2011153 e1-10.
Ranchoux, B., et al., 2015. Chemotherapy-induced pulmonary hypertension: role of alkylating agents. Am. J. Pathol. 185, 356–371. https://doi.org/10.1016/j.ajpath.2014.10.021.
Rennard, S.I., et al., 1986. Estimation of volume of epithelial lining fluid recovered by lavage using urea as marker of dilution. J. Appl. Physiol. 60, 532–538. https://doi.org/10.1152/jappl.1986.60.2.532, 1985.
Takahashi, M., et al., 2021. Effects of steric hindrance and electron density of ester prodrugs on controlling the metabolic activation by human carboxylesterase. Drug Metab. Pharmacokinet. 38, 100391. https://doi.org/10.1016/j.dmpk.2021.100391.